BIOCHEMISTRY
including biophysical chemistry & molecular biology

Accelerated Publication

pubs.acs.org/biochemistry

S_0-State Model of the Oxygen-Evolving Complex of Photosystem II

Rhitankar Pal,[†] Christian F. A. Negre,[†] Leslie Vogt,[†] Ravi Pokhrel,[†] Mehmed Z. Ertem,[†,‡] Gary W. Brudvig,*[,†] and Victor S. Batista*[,†]

[†]Department of Chemistry, Yale University, New Haven, Connecticut 06511, United States

[‡]Department of Chemistry, Brookhaven National Laboratory, Building 555A, Upton, New York 11973, United States

Supporting Information

ABSTRACT: The $S_0 \rightarrow S_1$ transition of the oxygen-evolving complex (OEC) of photosystem II is one of the least understood steps in the Kok cycle of water splitting. We introduce a quantum mechanics/molecular mechanics (QM/MM) model of the S_0 state that is consistent with extended X-ray absorption fine structure spectroscopy and X-ray diffraction data. In conjunction with the QM/MM model of the S_1 state, we address the proton-coupled electron-transfer (PCET) process that occurs during the $S_0 \rightarrow S_1$ transition, where oxidation of a Mn center and deprotonation of a μ-oxo bridge lead to a significant rearrangement in the OEC. A hydrogen bonding network, linking the D1-D61 residue to a Mn-bound water molecule, is proposed to facilitate the PCET mechanism.

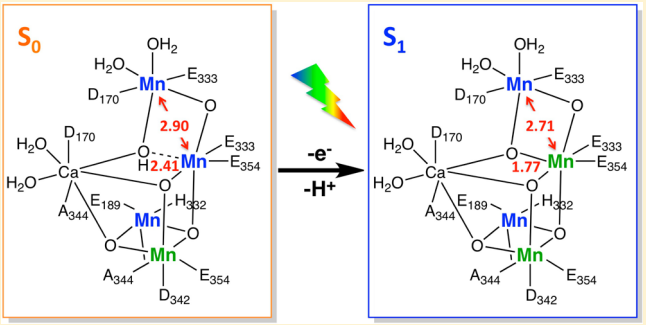

Photosystem II (PSII) is a 650 kDa protein complex found in the thylakoid membranes of higher plants, algae, and internal membranes of cyanobacteria. It is the only biological machinery that utilizes solar energy for water oxidation,[1−4] extracting reducing equivalents from water and generating molecular O_2 as a byproduct. The PSII complex consists of ∼20 protein subunits, numerous electron-transport cofactors, chlorophyll and β-carotene pigments, and a $CaMn_4O_5$ catalytic core, known as the oxygen-evolving complex (OEC).[5,6] In PSII, absorption of a photon triggers an efficient charge separation across the membrane bilayer, stabilizing the generation of a radical cation on a pair of chlorophylls, $P_{680}^{+\bullet}$. In the charge-separated state, $P_{680}^{+\bullet}$, with an estimated E° of 1.25 V, is the primary oxidant in PSII. In each step of the catalytic cycle, $P_{680}^{+\bullet}$ oxidizes a redox-active tyrosine residue (Y_Z), which in turn oxidizes the OEC. Four successive photo-oxidation steps are required for a complete cycle turnover, advancing the redox state of the OEC through five storage states (S states, S_i, where $i = 0-4$). The S_0 state is the most reduced state, and four sequential oxidations transform the OEC into the S_4 state. An O−O bond forms in the S_4 state, upon which the OEC relaxes back to the S_0 state. All but the $S_1 \rightarrow S_2$ oxidative transition involve the release of a proton to the lumen. Hence, efficient transfer of a proton from the OEC to the lumen is critical for redox leveling during successive oxidation steps in the S-state cycle. Therefore, elucidating the redox leveling mechanism in the oxidation of water at the OEC is of fundamental importance for the design of artificial systems capable of catalyzing the water oxidation reaction with a similar efficiency.

Biophysical studies based on time-resolved mass spectrometry,[7−9] electron paramagnetic resonance (EPR) spectroscopy,[10−12] Fourier transform infrared (FTIR) spectroscopy,[13−15] and X-ray diffraction (XRD),[16−20] as well as computational modeling,[21−28] have been instrumental in gaining structural and mechanistic insights. In particular, multiple research groups over the past decade have reported XRD models of PSII at progressively higher resolution (3.8−1.9 Å).[16−20] These breakthroughs in XRD have converged into a model of the OEC that involves a cuboidal $CaMn_3$ cluster with a dangling Mn held together by putative μ-oxo bridges and protein side chains. The model is consistent with earlier proposals based on EPR and extended X-ray absorption fine structure (EXAFS) spectroscopy.[11,29,30] The XRD model at 1.9 Å resolution has resolved for the first time terminal water molecules directly bound to Ca^{2+} and the dangling Mn.[20]

Several new features, including an additional μ-oxo bridge connecting the dangling Mn with the $CaMn_3O_4$ cube and D1-D170 as a bridging ligand between Ca^{2+} and the dangling Mn, were also resolved in the 1.9 Å XRD structure.[20] Furthermore, carboxylate ligands D1-E333, CP43-E354, and D1-D342 and the C-terminus of D1-A344 were shown to bridge the Mn and Ca^{2+} ions of the cluster (see Figure 1). The D1-E189 and D1-H332 side chains were shown to coordinate Mn1 directly. However, simulations of EXAFS spectra suggested that the XRD model of the OEC represents an average structure of the OEC in multiple oxidation states, including the states of the OEC more reduced than those present in the catalytic cycle of water splitting.[24,31] The XRD model has allowed the development of a quantum mechanics/molecular mechanics (QM/MM) model of the OEC

Received: September 3, 2013
Revised: October 10, 2013

   dx.doi.org/10.1021/bi401214v | *Biochemistry* XXXX, XXX, XXX−XXX

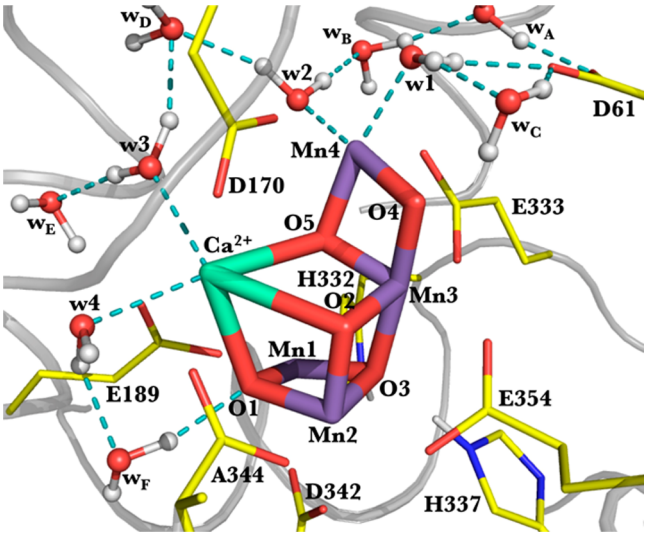

Figure 1. Quantum mechanics/molecular mechanics-optimized S_1-state structure of the OEC $CaMn_4O_5$ cluster, along with all directly ligated amino acid residues (D170, E189, H332, E333, H337, D342, A344, and E354), residue D61, and 10 water molecules forming crucial hydrogen bonding networks. Four water molecules are directly ligated to the OEC (w1−w4), and six others (labeled w_A−w_F) are in the second sphere.

in the S_1 Mn_4[III,IV,IV,III] state that is consistent with X-ray data, showing that Ca^{2+} is bridged to Mn by the carboxylate moieties of D170 and A344, and with high-resolution spectroscopy, including polarized EXAFS data of oriented single crystals.[24] While several density functional theory (DFT) models for the S_0 state have been suggested,[21−23] a structural model that is fully consistent with EXAFS and XRD data has yet to be reported. In conjunction with the previously reported QM/MM S_1 model,[24] the S_0 structure would provide a mechanistic proposal for the $S_0 \rightarrow S_1$ transition in which oxidation of a Mn ion and deprotonation of a μ-hydroxo bridge lead to significant rearrangements in the OEC.

Using QM/MM optimizations followed by Monte Carlo (MC) refinements, as in our prior work, we propose an S_0 model, which suggests that the $S_0 \rightarrow S_1$ PCET mechanism could involve deprotonation of the O5 μ-hydroxo bridge via hydrogen-bonded water molecules linking Mn4 and the D1-D61 residue. Furthermore, we demonstrate that the structural models obtained with this approach for the S_1 and S_0 states are consistent with both EXAFS[29] and XRD[20] data.

The QM/MM models were built using a two-layer ONIOM link H-atom approach implemented in Gaussian09,[32] as in our previous studies.[24,26,27] However, in this work, we expanded the QM region to move the QM/MM boundary farther from the OEC and to better model the hydrogen bonding network surrounding the cluster. The S_1 model has been reoptimized with this expanded QM region for the sake of comparison. The QM layer includes the OEC, all directly ligated side chains (D1-D170, D1-E189, D1-H332, D1-E333, D1-D342, and CP43-E354), the C-terminus of D1-A344, hydrogen-bonded residues D1-H337 and CP43-R357, residue D1-D61, and 10 water molecules shown in Figure 1 (further details are provided in section I of the Supporting Information). The MM layer includes all residues with Cα atoms within 15 Å of the OEC, crystallographic waters within this boundary, two chloride ions, and amino acids that span gaps of up to two residues in the peptide chains of the main selection (section I of the Supporting Information). QM/MM optimizations were performed using the B3LYP[33,34] functional with the LANL2DZ[35,36] pseudopotential for Ca and Mn and the 6-31G*[37] basis set for all other atoms. The AMBER force field[38] was used for all MM layer atoms. EXAFS spectra were calculated using the *ab initio* real space Green's function approach as implemented in FEFF (version 8.30).[39] EXAFS structural refinement was based on simulated annealing MC (see section I of the Supporting Information), fully relaxing the geometry of the $CaMn_4O_5$ cluster, and relaxing all the directly coordinated ligands with harmonic constraints relative to the QM/MM-optimized positions (R-QM/MM).

The calculated EXAFS for the reoptimized QM/MM S_1 model agrees very well with the experimental spectrum (Figure S3 of the Supporting Information). It is important to note that the optimization of the isolated DFT model layer leads to a worse match for the EXAFS spectrum and requires larger displacements in the MC refinement (section II and Figure S4 of the Supporting Information). Therefore, the advantage of performing QM/MM optimization rather than using a DFT cluster model is clearly reflected in the better agreement with the experimental EXAFS spectrum, which is also consistent with the recent findings of Retegan et al.[28]

Having a reasonable structure of the S_1 state using QM/MM optimization, we used this approach to investigate the structure of the S_0 state. To determine the likely site for protonation of the OEC in the S_0 state, a preliminary MC screening using a simulated annealing algorithm[40] was performed on the geometry of the S_1 model to fit the S_0 EXAFS data. MC optimization revealed that the Mn3, Mn4, O4, and O5 atoms of the OEC had significant displacements, thereby suggesting possible protonation at the O5 or O4 μ-oxo bridges in the S_0 state (see the Supporting Information for further details). Furthermore, this also indicated that either Mn3 or Mn4 must be oxidized during this transition to induce the requisite geometry change. These results are in agreement with the reported *B* factors of the atoms in the X-ray crystal structure at 1.9 Å resolution (Protein Data Bank entry 3ARC).[20] The other μ-oxo atoms are unlikely to be protonated as O2 is near the positively charged R357 and O3 is strongly hydrogen bonded to H337. In light of these observations, we explored the protonation of O4 and O5 sites using our QM/MM model of the S_0 state. The EXAFS spectra of the O4−H and O5−H models (QM/MM and R-QM/MM) are shown in Figure 2. An overlay of the QM/MM and R-QM/MM structures of the S_0 state where either O5 or O4 is protonated is shown in Figure S6 (section IV of the Supporting Information).

The intermetallic distances listed in Table 1 for the S_0 and S_1 QM/MM models provide a clear description of the underlying structural rearrangements induced by the $S_0 \rightarrow S_1$ oxidation-state transition. In the S_0 state, the formal oxidation number of Mn3 is III, and upon oxidation to the S_1 state, the formal oxidation number of Mn3 increases to IV. This shortens the Mn3−O5 distance, inducing deprotonation of the O5−H μ-hydroxo bridge and shortening the Mn3−Mn4 distance from 2.9 to 2.7 Å (Figure 3, top panel). As a result, the S_1 model has three short Mn−Mn distances of ∼2.7 Å (Mn1−Mn2, Mn2−Mn3, and Mn3−Mn4) and a long Mn1−Mn3 distance of ∼3.2 Å.

In contrast, the S_0 model has only two short Mn−Mn distances of ∼2.7 Å (Mn1−Mn2 and Mn2−Mn3), while the other two Mn−Mn distances (i.e., Mn1−Mn3 and Mn3−Mn4) are longer (∼2.9−3.0 Å). The elongated Mn3−Mn4 distance in the S_0 state is the major difference between the S_0 and S_1 models (Figure 3) and is clearly manifested in the comparison of Fourier transform EXAFS spectra (Figure 3, bottom panel). In the 2.0−3.0 Å region

dx.doi.org/10.1021/bi401214v | *Biochemistry* XXXX, XXX, XXX−XXX

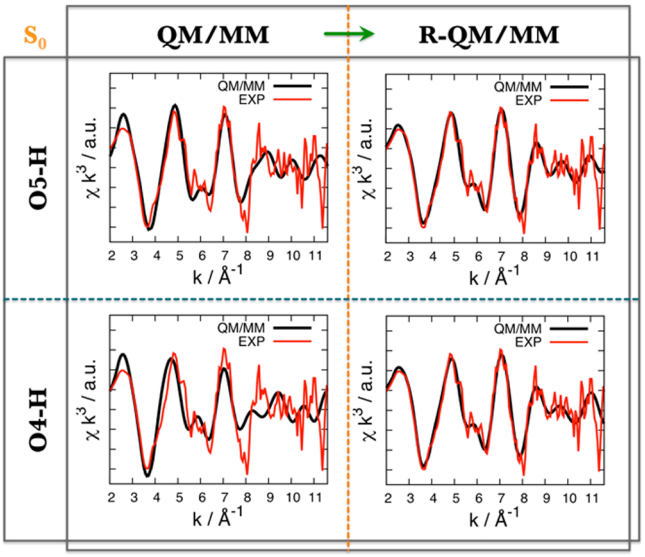

Figure 2. Comparison of the experimental EXAFS spectrum for the OEC S_0 state[29] and the calculated spectra based on the DFT-QM/MM (left) and R-QM/MM (right) models with μ-hydroxo bridges at O5 (top) and O4 (bottom).

Table 1. Intermetallic Distances (in angstroms) in the X-ray Structure[20] and in the R-QM/MM Models of the S_0 (O5 protonated) and S_1 States

	X-ray	S_1	S_0 O5−H
	chain A/a	QM/MM (R-QMMM)	QM/MM (R-QMMM)
Mn1−Mn2	2.84/2.76	2.73 (2.74)	2.72 (2.74)
Mn1−Mn3	3.29/3.30	3.26 (3.27)	3.20 (3.19)
Mn1−Mn4	5.00/4.95	4.76 (4.70)	4.72 (4.66)
Mn2−Mn3	2.89/2.91	2.76 (2.75)	2.77 (2.76)
Mn2−Mn4	5.44/5.37	5.02 (5.02)	5.25 (5.19)
Mn3−Mn4	2.97/2.91	2.68 (2.71)	2.95 (2.90)
Ca^{2+}−Mn1	3.51/3.46	3.55 (3.52)	3.37 (3.41)
Ca^{2+}−Mn2	3.36/3.29	3.44 (3.50)	3.46 (3.45)
Ca^{2+}−Mn3	3.41/3.44	3.58 (3.65)	3.72 (3.73)
Ca^{2+}−Mn4	3.79/3.80	3.68 (3.70)	3.92 (3.91)

of reduced distance, a single peak in the S_1 state splits into a doublet in the S_0 state (Figure 3, bottom panel, and section VI of the Supporting Information).

Recent experimental observations suggest that the oxidation of the OEC precedes the release of the proton to the lumen, during the $S_0 \rightarrow S_1$ transition, unlike the later S-state transitions in which proton release occurs prior to oxidation of the OEC.[41] However, the detailed mechanism responsible for the translocation of the proton to the lumen has yet to be established.

We have analyzed the possibility of a Grotthuss-like mechanism[42] for deprotonation during the $S_0 \rightarrow S_1$ transition in which D1-D61 is involved in the transfer of the proton to the lumen.[26,27,43] We examined the removal of the proton from the O5−H hydroxo bridge, via the w2 → w_B → w_A → D61 pathway. In the QM/MM S_0 model, the hydroxo bridge of O5 does not form a direct hydrogen bond with any of the OEC-bound or second-shell water molecules. However, we find that a water ligand of the dangling Mn (w2) could function as a proton acceptor after deprotonation (Figure S7 of the Supporting Information). To test this hypothesis, an S_0' model was constructed by oxidizing the Mn3 center (III → IV) and

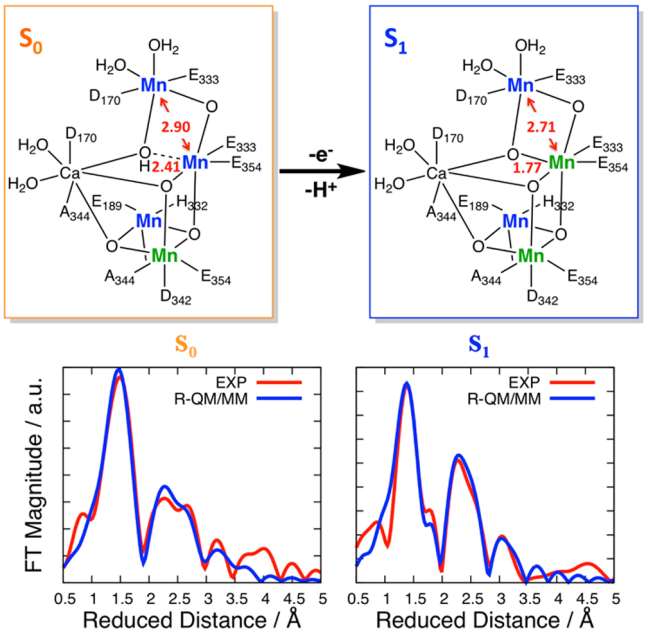

Figure 3. Structural changes induced by the $S_0 \rightarrow S_1$ transition (top). The Mn3−Mn4 and Mn3−O5 distances are shortened upon oxidation of Mn and deprotonation of the hydroxo bridge: green for Mn^{IV} and blue for Mn^{III}. Comparison of the experimental Fourier transform EXAFS spectra (red) and the calculated (blue) spectra of the S_0 (left) and S_1 (right) QM/MM models (bottom).

deprotonating the w2 molecule (Figure S7b of the Supporting Information), which can be facilitated by the hydrogen bonding network connecting w2 to the D1-D61 side chain. The DFT calculations indicate that the hydroxo ligand of Mn4 could deprotonate the O5−H μ-hydroxo bridge through a barrierless and thermodynamically spontaneous process. The energetics of removal of the proton from O5−H to w2(OH^-) was computed by increasing the O5−H bond length from 1.1 to 2.3 Å and relaxing the entire model at every step. The overall path was found to be exothermic by ~17 kcal/mol (see section VI of the Supporting Information for details).

In summary, we conclude that the $S_0 \rightarrow S_1$ transition of the OEC of PSII involves oxidation of Mn3 (from III to IV) and deprotonation of the O5−H μ-hydroxo bridge. The oxidation reduces the Mn3−Mn4 intermetallic distance from 2.9 to 2.7 Å because of the removal of the Jahn−Teller distortion. This structural/oxidation-state transition strengthens the Mn3−O5 bond, leading to deprotonation of the OH ligand. The resulting structural rearrangements of the Mn cluster are fully consistent with the EXAFS spectroscopy of the S_0- and S_1-state intermediates. Deprotonation of the O5−H μ-hydroxo bridge is likely mediated by a Grotthuss-like proton-transport mechanism that involves a stable hydrogen bonding network linking w2 and D1-D61 via bound water molecules w_B and w_A.

■ ASSOCIATED CONTENT

Supporting Information

Description of computational methods, pictorial representation of the X-ray structure β factors on the atoms of the metal cluster at the center of the OEC, combined MC-DFT-generated EXAFS, and coordinates of the QM/MM and MC-refined models. This material is available free of charge via the Internet at http://pubs.acs.org.

dx.doi.org/10.1021/bi401214v | *Biochemistry* XXXX, XXX, XXX−XXX

AUTHOR INFORMATION

Corresponding Authors

*E-mail: victor.batista@yale.edu. Phone: (203) 432-6672. Fax: (203) 432 6144.

*E-mail: gary.brudvig@yale.edu. Phone: (203) 432-5202. Fax: (203) 432-6144.

Funding

Notes

The authors declare no competing financial interest.

ACKNOWLEDGMENTS

V.S.B. acknowledges supercomputer time from NERSC and financial support from the Division of Chemical Sciences, Geosciences, and Biosciences, Office of Basic Energy Sciences, U.S. Department of Energy (DESC0001423. Biochemical work was supported by the Department of Energy, Office of Basic Energy Sciences, Division of Chemical Sciences (Grant DE-FG02-05ER15646 to G.W.B.). M.Z.E. was funded by a Computational Materials and Chemical Sciences (CMCSN) project at Brookhaven National Laboratory under contract DE-AC02-98CH10886 with the U.S. DOE and supported by its Division of Chemical Sciences, Geosciences & Biosciences, Office of Basic Energy Sciences.

REFERENCES

(1) Debus, R. J. (1992) *Biochim. Biophys. Acta 1102*, 269−352.

(2) Dau, H., and Haumann, M. (2008) *Coord. Chem. Rev. 252*, 273−295.

(3) Lubitz, W., Reijerse, E. J., and Messinger, J. (2008) *Energy Environ. Sci. 1*, 15−31.

(4) Vinyard, D. J., Ananyev, G. M., and Dismukes, G. C. (2013) *Annu. Rev. Biochem. 82*, 577−606.

(5) Kashino, Y., Lauber, W. M., Carroll, J. A., Wang, Q., Whitmarsh, J., Satoh, K., and Pakrasi, H. B. (2002) *Biochemistry 41*, 8004−8012.

(6) McEvoy, J. P., and Brudvig, G. W. (2006) *Chem. Rev. 106*, 4455−4483.

(7) Messinger, J., Badger, M., and Wydrzynski, T. (1995) *Proc. Natl. Acad. Sci. U.S.A. 92*, 3209−3213.

(8) Hillier, W., and Wydrzynski, T. (2004) *Phys. Chem. Chem. Phys. 6*, 4882−4889.

(9) Hillier, W., and Wydrzynski, T. (2008) *Coord. Chem. Rev. 252*, 306−317.

(10) Peloquin, J. M., Campbell, K. A., Randall, D. W., Evanchik, M. A., Pecoraro, V. L., Armstrong, W. H., and Britt, R. D. (2000) *J. Am. Chem. Soc. 122*, 10926−10942.

(11) Britt, R. D., Campbell, K. A., Peloquin, J. M., Gilchrist, M. L., Aznar, C. P., Dicus, M. M., Robblee, J., and Messinger, J. (2004) *Biochim. Biophys. Acta 1655*, 158−171.

(12) Kulik, L. V., Epel, B., Lubitz, W., and Messinger, J. (2005) *J. Am. Chem. Soc. 127*, 2392−2393.

(13) Chu, H. A., Hillier, W., and Debus, R. J. (2004) *Biochemistry 43*, 3152−3166.

(14) Debus, R. J. (2008) *Coord. Chem. Rev. 252*, 244−258.

(15) Noguchi, T. (2008) *Coord. Chem. Rev. 252*, 336−346.

(16) Zouni, A., Witt, H. T., Kern, J., Fromme, P., Krauss, N., Saenger, W., and Orth, P. (2001) *Nature 409*, 739−743.

(17) Ferreira, K. N., Iverson, T. M., Maghlaoui, K., Barber, J., and Iwata, S. (2004) *Science 303*, 1831−1838.

(18) Loll, B., Kern, J., Saenger, W., Zouni, A., and Biesiadka, J. (2005) *Nature 438*, 1040−1044.

(19) Guskov, A., Kern, J., Gabdulkhakov, A., Broser, M., Zouni, A., and Saenger, W. (2009) *Nat. Struct. Mol. Biol. 16*, 334−342.

(20) Umena, Y., Kawakami, K., Shen, J. R., and Kamiya, N. (2011) *Nature 473*, 55−60.

(21) Isobe, H., Shoji, M., Yamanaka, S., Umena, Y., Kawakami, K., Kamiya, N., Shen, J. R., and Yamaguchi, K. (2012) *Dalton Trans. 41*, 13727−13740.

(22) Siegbahn, P. E. (2013) *Biochim. Biophys. Acta 1827*, 1003−1019.

(23) Ichino, T., and Yoshioka, Y. (2012) *Chem. Phys. Lett. 545*, 107−111.

(24) Luber, S., Rivalta, I., Umena, Y., Kawakami, K., Shen, J. R., Kamiya, N., Brudvig, G. W., and Batista, V. S. (2011) *Biochemistry 50*, 6308−6311.

(25) Sproviero, E. M., Gascon, J. A., McEvoy, J. P., Brudvig, G. W., and Batista, V. S. (2006) *J. Chem. Theory Comput. 2*, 1119−1134.

(26) Sproviero, E. M., Gascon, J. A., McEvoy, J. P., Brudvig, G. W., and Batista, V. S. (2008) *J. Am. Chem. Soc. 130*, 3428−3442.

(27) Sproviero, E. M., Gascon, J. A., McEvoy, J. P., Brudvig, G. W., and Batista, V. S. (2008) *J. Am. Chem. Soc. 130*, 6728−6730.

(28) Retegan, M., Neese, F., and Pantazis, D. A. (2013) *J. Chem. Theory Comput. 9*, 3832−3842.

(29) Haumann, M., Muller, C., Liebisch, P., Iuzzolino, L., Dittmer, J., Grabolle, M., Neisius, T., Meyer-Klaucke, W., and Dau, H. (2005) *Biochemistry 44*, 1894−1908.

(30) Grabolle, M., Haumann, M., Muller, C., Liebisch, P., and Dau, H. (2006) *J. Biol. Chem. 281*, 4580−4588.

(31) Galstyan, A., Robertazzi, A., and Knapp, E. W. (2012) *J. Am. Chem. Soc. 134*, 7442−7449.

(32) Frisch, M. J., et al. (2009) *Gaussian 09*, Gaussian, Inc., Wallingford, CT.

(33) Becke, A. D. (1988) *Phys. Rev. A 38*, 3098−3100.

(34) Becke, A. D. (1993) *J. Chem. Phys. 98*, 5648−5652.

(35) Wadt, W. R., and Hay, P. J. (1985) *J. Chem. Phys. 82*, 284−298.

(36) Hay, P. J., and Wadt, W. R. (1985) *J. Chem. Phys. 82*, 299−310.

(37) Hariharan, P. C., and Pople, J. A. (1973) *Theor. Chim. Acta 28*, 213−222.

(38) Case, D. A., et al. (2012) *AMBER 12*, University of California, San Francisco.

(39) Ankudinov, A. L., Bouldin, C. E., Rehr, J. J., Sims, J., and Hung, H. (2002) *Phys. Rev. B 65*, 104107.

(40) Kirkpatrick, S., Gelatt, C. D., and Vecchi, M. P. (1983) *Science 220*, 671−680.

(41) Klauss, A., Haumann, M., and Dau, H. (2012) *Proc. Natl. Acad. Sci. U.S.A. 109*, 16035−16040.

(42) Cukierman, S. (2006) *Biochim. Biophys. Acta 1757*, 876−885.

(43) Service, R. J., Hillier, W., and Debus, R. J. (2010) *Biochemistry 49*, 6655−6669.

NOTE ADDED AFTER ASAP PUBLICATION

This paper published ASAP on October 17, 2013. The Supporting Information file was replaced and the revised version was reposted on October 21, 2013.